

See discussions, stats, and author profiles for this publication at: <https://www.researchgate.net/publication/51470608>

Orthogonally Dual-Clickable Janus Nanoparticles via a Cyclic Templating Strategy

ARTICLE *in* JOURNAL OF THE AMERICAN CHEMICAL SOCIETY · JULY 2011

Impact Factor: 12.11 · DOI: 10.1021/ja203133h · Source: PubMed

CITATIONS

36

READS

27

6 AUTHORS, INCLUDING:



Guorong Sun

Texas A&M University

28 PUBLICATIONS 784 CITATIONS

SEE PROFILE



Karen L Wooley

Texas A&M University

327 PUBLICATIONS 17,723 CITATIONS

SEE PROFILE

Published in final edited form as:

J Am Chem Soc. 2011 July 27; 133(29): 11046–11049. doi:10.1021/ja203133h.

Orthogonally dual-clickable Janus nanoparticles *via* a cyclic templating strategy

Shiyi Zhang^{†,‡}, Zhou Li^{†,‡}, Sandani Samarajeewa[†], Guorong Sun[†], Chao Yang[†], and Karen L. Wooley^{†,‡,*}

[†]Departments of Chemistry and Chemical Engineering, Texas A&M University, College Station, Texas, 77842

[‡]Department of Chemistry, Washington University in St. Louis, St. Louis, Missouri, 63130

Abstract

Synthetic asymmetrical systems, Janus particles and patchy particles, are capable of undergoing hierarchical assembly processes that mimic those of Nature, to serve as switchable devices, optical probes, phase-transfer catalysts and multi-functional drug carriers, each of which benefits from opposing surface patterns behaving differently. Production of nanometer-sized Janus particles that are equipped with efficient chemistries remains a challenge. A robust Janus-faced polymer nanoparticle framework that presents two orthogonally click-reactive surface chemistries, has been generated by a recyclable strategy that involves reactive functional group transfer by templating against gold nanoparticle substrates. This anisotropic functionalization approach is compatible with a wide range of soft materials, providing Janus nanoparticles for the construction of dual-functionalized devices by accurately controlling chemical functionality at the nanoscopic level.

Inspired by the many selective, hierarchical assembly processes that afford complex materials in Nature, the directional organization of Janus particles into complex structures has attracted much attention.^{1,2} Beyond fundamental studies, the differentiation of chemistries across the surface regions of Janus nanoparticles could lead to their development as components in the construction of switchable devices,³ optical probes,⁴ phase-transfer catalysts,⁵ multi-functional drug carriers,⁶ and other applications, each of which could benefit from the different surface functionalities being featured in an efficient and orthogonal way.⁷ During the past decade, “click chemistry”⁸ has provided a library of chemical reactions for the preparation and functionalization of new soft materials, based on robust, efficient, and orthogonal chemistries.⁹ At the current stage, limited approaches are available for the production of microscopic Janus particles carrying one kind of click chemistry for efficient chemical modification.^{10,11} As we have a keen interest in highly complex nanomaterials, we have developed an economically-efficient, cyclic strategy to produce nanoscopic Janus particles that bear two kinds of clickable surface functional groups (thiol and azide), while also being comprised of an amphiphilic core-shell morphology, illustrated in Fig. 1, A. Therefore, the differentiations of chemistry proceed about the external surface of the nanoparticles and also concentrically within their internal region.

The cyclic nano-patterning process involved covalent attachment of pre-established amphiphilic core-shell polymer nanoparticles (shell crosslinked knedel-like (SCK)

Corresponding Author Tel. (979) 845-4077 Fax (979) 862-1137, wooley@chem.tamu.edu.

Supporting Information. Detailed experimental section, TEM images, AFM images, DLS histograms, and ref 2f full author listing. This material is free of charge via the Internet at <http://pubs.acs.org>.

nanoparticles) onto inorganic nanoparticle substrates, followed by their displacement by a manner that resulted in the chemical modification of the contact portion of the SCKs, with coincident regeneration of the template (Figure 1a). In the first step of this cycle, the uniformly azide-functionalized polymer nanoparticles ($D_n = 22 \pm 3$ nm) were attached onto alkyne-functionalized gold nanoparticles (GNPs) ($D_n = 46 \pm 6$ nm) to form hybrid nanoclusters by aqueous click reactions (Figure 1b). After separation (step 2, Figure 1c), the SCKs were detached from the GNPs with the assistance of ligand exchange by breaking the Au-S bonds (step 3) and replacing the consumed alkynyl ligands. The resulting azide-functionalized SCKs contained a patch of thiol groups (with the possibility of residual azides also being present within this templated domain); meanwhile, the alkyne-functionalized GNPs were recovered and recycled as multi-use nano-templates (step 4). The anisotropic distribution of thiol groups on the SCK surfaces and the orthogonality of the two clickable functionalities were then demonstrated.

By our approach, preparation of the Janus nanoparticles within the desymmetrization cycle, in which thiol groups were introduced onto one surface of the azide-functionalized SCKs by covalent transfer of alkyne-oligo(ethylene oxide)-thiol units from the GNPs, required establishment of each of the GNP template and the functionalizable SCK. The alkyne-OEO-thiol-functionalized GNPs that serve as the clickable template were prepared (Scheme. 1a) according to a previously reported well-established protocol.¹² We also prepared its counterpart (see methods), the azide-functionalized SCKs (Scheme. 1b) through self assembly of amphiphilic poly(acrylic acid)-*block*-polystyrene (PAA₁₀₅-*b*-PS₁₃₅) block copolymers in water, followed by azide functionalization and intra-micellar crosslinking. The post-micellization chemical modification technique using hydrophilic ethyleneoxy repeating units of 11-azido-3,6,9-trioxaundecan-1-amine was chosen to increase the flexibility and availability of azide functionalities on the surface of the micelles and SCKs. Azide-functionalized micelles were then crosslinked, to afford the robust SCKs, which are stable,¹³ biocompatible,¹⁴ and capable of being loaded with hydrophobic guest molecules for controlled release purposes.¹⁵

Although click chemistry has been widely used in bio- and nano-science technologies, there are few examples¹⁶ in which two kinds of nanoparticles act as substrates. Click reactions carried out between azide-functionalized SCKs and alkyne-functionalized GNPs represent a new direction to engineer surface-functionalized nanostructures toward tailor-made complex architectures with hybrid composites in the field of nanotechnology. Due to the multi-functional nature of the two nanoparticle surfaces, crosslinked networks were generated initially by Cu-catalyzed azide/alkyne cycloaddition (CuAAC) reactions (Supplementary Fig. S1). For instance, visible precipitation was observed when a near 1:1 ratio of clickable nanoparticles was allowed to undergo reaction, whereas interparticle crosslinking was suppressed when the feed ratio of SCKs to GNPs was increased to *ca.* 500:1. As a result, those SCKs that were attached to GNPs had only one surface binding to the GNPs. The transmission electron microscopy (TEM) images clearly showed hybrid nanocluster satellite structures,¹⁷ consisting of one GNP surrounded by several SCKs, together with populations of unbound SCKs (Fig. 1b). It is noteworthy that the binding capacity of SCKs onto GNPs allows for production of dual-clickable Janus SCKs at levels that far exceed the quantity of materials and cyclability than could be achieved on a planar two-dimensional substrate.¹⁸ It is calculated that as many as 27 SCKs can be accommodated onto each GNP, according to the geometry and relative size of these two particles (Supplementary Fig. S2). The hybrid nanoclusters could be isolated from unbound SCKs by ultracentrifugation (Fig. 1c and Fig. S3, S4). The recovered SCKs were then collected and purified by dialysis for recycling.

The hybrid nanoclusters were then dismantled to provide the dual-clickable Janus SCKs and to regenerate the nano-template alkyne-functionalized GNPs. During the ligand-exchange

reaction,¹⁹ SCKs were detached from GNPs after excess alkyne-OEO-thiol was added. After Au-S bonds in the hybrid nanoclusters were broken, the detached SCKs contained a patch of thiol functionalities. Ultracentrifugation was applied to separate the Janus-faced SCKs (JSCKs) from the alkyne-functionalized GNPs by taking advantage of their different densities. Each step of the desymmetrization cycle was monitored by ultraviolet-visible spectroscopy (UV-vis) measurements of the gold surface plasmon resonance band in the solution, which reflects the surface functionality of GNPs. As observed from UV-vis, dynamic light scattering (DLS) and TEM (Fig. S5), the recovered alkyne-functionalized GNPs were of comparable size, shape and surface functionality to the freshly-synthesized GNPs. The recovered alkyne-functionalized GNPs were, therefore, reused to desymmetrize another batch of SCKs. This cyclic approach (Fig. 1a) greatly enhances the atom efficiency of the solid phase synthesis strategy, which is widely used to desymmetrize and regionally functionalize microparticles and nanoparticles,²⁰ and has a potential for large scale synthesis of Janus nanoparticles by using recyclable nanoscopic templates rather than singly-used templates. In our approach, as the nano-template can be recovered and reused in an economical cyclic manner, it can be applied to other soft matter particles with various sizes and compositions.

To confirm the anisotropic distribution of thiol groups on the resultant JSCKs, the thiol-functionalized regions of JSCKs were labeled with 2 nm citrate-stabilized GNPs. As revealed by TEM analyses (Fig. 2a), a relatively high population of JSCKs, 72% by counting more than 100 JSCKs, was attached to one or two 2 nm GNPs on one side, where thiol functionalities were expected. These TEM images strongly suggest the Janus nature of JSCKs and confirm the anisotropic distribution of thiol functionalities. Additionally, these JSCKs were found to undergo attachment of three or even more GNPs on one surface (Supplementary Fig. S7). Negative and positive control experiments were conducted based upon uniformly azide- or thiol-functionalized SCKs, respectively.²¹ The negative control experiment demonstrated that citrate-stabilized GNPs did not interact favorably with azide-functionalized SCK nanoparticles (Fig. S6, b and e). In the positive control experiment, thiol-functionalized SCKs had strong tendency to form aggregates and undergo precipitation, due to the formation of disulfide bonds between SCKs upon oxidation;²² in contrast, JSCKs showed no precipitation as a result of only few thiol groups functionalized on one side of each nanoparticle. Meanwhile, the GNPs were attached onto multiple places of homogeneously thiol-functionalized SCKs, but didn't undergo close-packing to cover the entire surface (Fig. S6, c and f). These phenomena can be attributed to steric effects and static repulsion among GNPs. Therefore, it is expected that there are more thiol groups on the JSCKs than it appears.

Two types of click reactions were conducted, CuAAC and thiol-maleimide Michael addition, to demonstrate the presence and chemical availability of azide and thiol groups on the JSCKs. Alkyne-functionalized fluorescein was conjugated onto the residual azides of the JSCKs in the presence of CuSO₄/sodium ascorbate catalyst in water, followed by installation of thiol-reactive BODIPY 577/618 maleimide onto the thiol-functionalized patches on the JSCKs, by reaction in sodium carbonate buffered solution. After removal of the excess unreacted dyes, the presence of the two click-reactive dyes coupled onto JSCKs was studied by pH-dependent fluorescence experiments (Fig. 3) and their amounts were quantified by UV-vis spectroscopy.²³ The ratio of fluorescein to BODIPY was calculated as 5:1, which indicated that *ca.* 17% of the azide groups on the SCKs were substituted by thiol groups, under the assumption of quantitative conversion and yield for the click reactions.²⁴ Such orthogonality and efficiency of click chemistry together with the Janus nature will allow for precise functionalization of polymer nanoparticles with targeted biological moieties, such as peptides, proteins, enzymes, and viral systems, to produce multifunctional synthetic polymer-biological chimeras for sophisticated applications. This JSCK system is currently

being extended to load with a pair of FRET dyes, which will provide additional information to further understand the distribution of azide and thiol groups.

In comparison to SCKs, the results of click reaction between azide-functionalized micelles and alkyne-functionalized GNPs were unsatisfactory. As illustrated by TEM imaging (Fig. S8a), five days after micelles were attached onto GNPs, the boundaries between different micelles became indistinct and eventually disappeared to form a polymer layer coated on the GNPs.²⁵ The polymer encapsulated GNP aggregates may be responsible for the red shift observed in UV-Vis spectra and micron-sized particle distribution as detected by DLS (Supplementary Fig. S8, b and c). Upon adsorption and attachment of the polymer micelles onto the GNPs, the changes in local concentration and surface forces serve as stimuli to trigger the disassembly and reorganization of block copolymers. Therefore, the micelles could be taken no further in the process toward Janus nanostructures. The robustness should be taken into consideration when engineering self-assembled nanostructures toward hierarchical architectures. Chemical cross-linking is an efficient protocol to overcome this impediment and facilitate the “bottom-up” fabrication of self-assembled nanostructures.²⁶

In summary, we have demonstrated a novel, efficient and cyclic approach to construct orthogonal dual-clickable Janus nanoparticles, through a desymmetrization cycle based on complementarily reactive nanoscopic templates and covalent pattern transfer. The robustness of nanostructures is critical in this approach. This strategy can be further expanded as a general route to desymmetrize and dual-functionalize a large family of soft matter nanoparticles for anisotropic modification toward complex devices.

Supplementary Material

Refer to Web version on PubMed Central for supplementary material.

Acknowledgments

We gratefully acknowledge financial support from the National Heart Lung and Blood Institute of the National Institutes of Health as a Program of Excellence in Nanotechnology (HHSN268201000046C) and the National Science Foundation under grant numbers DMR-0906815 and DMR-1032267. The Welch Foundation is gratefully acknowledged for support through the W. T. Doherty-Welch Chair in Chemistry, Grant No. A-0001. The transmission electron microscopy facilities at Washington University in St. Louis, Department of Otolaryngology, Research Center for Auditory and Visual Studies funded by NIH P30 DC004665 are gratefully acknowledged. We thank J. Zhu and A. Li for discussions and support.

References

1. For reviews about soft Janus particles: (a) Wurm F, Kilbinger AFM. *Angew Chem Int Edit*. 2009; 48:8412.. (b) Du JZ, O'Reilly RK. *Chem Soc Rev*. 2011; 40:2402. [PubMed: 21384028] . (c) Walther A, Muller AHE. *Soft Matter*. 2008; 4:663.
2. (a) Glotzer SC. *Science*. 2004; 306:419. [PubMed: 15486279] (b) Walther A, Drechsler M, Rosenfeldt S, Harnau L, Ballauff M, Abetz V, Muller AHE. *J Am Chem Soc*. 2009; 131:4720. [PubMed: 19284726] (c) Hermans TM, Broeren MAC, Gomopoulos N, van der Schoot P, van Genderen MHP, Sommerdijk NAJM, Fytas G, Meijer EW. *Nat Nanotechnol*. 2009; 4:721. [PubMed: 19893514] (d) Roh K-H, Martin DC, Lahann J. *Nat Mater*. 2005; 4:759. [PubMed: 16184172] (e) Chen Q, Bae SC, Granick S. *Nature*. 2011; 469:381. [PubMed: 21248847] (f) Percec V, et al. *Science*. 2010; 328:1009. [PubMed: 20489021] (g) Chen T, Yang M, Wang X, Tan LH, Chen H. *J Am Chem Soc*. 2008; 130:11858. [PubMed: 18707100]
3. Berger S, Synytska A, Ionov L, Eichhorn KJ, Stamm M. *Macromolecules*. 2008; 41:9669.
4. Wu LY, Ross BM, Hong S, Lee LP. *Small*. 2010; 6:503. [PubMed: 20108232]
5. Crossley S, Faria J, Shen M, Resasco DE. *Science*. 2010; 327:68. [PubMed: 20044571]
6. Suci PA, Kang S, Young M, Douglas T. *J Am Chem Soc*. 2009; 131:9164. [PubMed: 19522495]

7. Gillies ER, Fréchet JMJ. *J Am Chem Soc.* 2002; 124:14137. [PubMed: 12440912]
8. Kolb HC, Finn MG, Sharpless KB. *Angew Chem Int Edit.* 2001; 40:2004.
9. Iha RK, Wooley KL, Nystrom AM, Burke DJ, Kade MJ, Hawker CJ. *Chem Rev.* 2009; 109:5620. [PubMed: 19905010]
10. Chen RT, Muir BW, Such GK, Postma A, McLean KM, Caruso F. *Chem Commun.* 2010; 46:5121.
11. Zhang J, Wang XJ, Wu DX, Liu L, Zhao HY. *Chem Mater.* 2009; 21:4012.
12. Elghanian R, Storhoff JJ, Mucic RC, Letsinger RL, Mirkin CA. *Science.* 1997; 277:1078. [PubMed: 9262471]
13. Thurmond KB, Kowalewski T, Wooley KL. *J Am Chem Soc.* 1996; 118:7239.
14. Sun G, Hagooley A, Xu J, Nystrom AM, Li ZC, Rossin R, Moore DA, Wooley KL, Welch MJ. *Biomacromolecules.* 2008; 9:1997. [PubMed: 18510359]
15. Lin LY, Lee NS, Zhu J, Nyström AM, Pochan DJ, Dorshow RB, Wooley KL. *J Control Release.* 2011; 152:37. [PubMed: 21241750]
16. Dach BI, Rengifo HR, Turro NJ, Koberstein JT. *Macromolecules.* 2010; 43:6549.
17. (a) Huo FW, Lytton-Jean AKR, Mirkin CA. *Adv Mater.* 2006; 18:2304. Xu X, Rosi NL. (b) Wang Y, Huo F, Mirkin CA. *J Am Chem Soc.* 2006; 128:9286. [PubMed: 16848436]
18. Lattuada M, Hatton TA. *J Am Chem Soc.* 2007; 129:12878. [PubMed: 17910450]
19. Latham AH, Williams ME. *Langmuir.* 2006; 22:4319. [PubMed: 16618182]
20. (a) Worden JG, Shaffer AW, Huo Q. *Chem Commun.* 2004:518. (b) Wang BB, Li B, Zhao B, Li CY. *J Am Chem Soc.* 2008; 130:11594. [PubMed: 18693735] (c) Maye MM, Nykypanchuk, Cuisinier M, van der Lelie D, Gang O. *Nature Mater.* 2009; 8:388. [PubMed: 19329992] (d) Sardar R, Heap TB, Shumaker-Parry JS. *J Am Chem Soc.* 2007; 129:5356. [PubMed: 17425320]
21. Takahara YK, Ikeda S, Ishino S, Tachi K, Ikeue K, Sakata T, Hasegawa T, Mori H, Matsumura M, Ohtani B. *J Am Chem Soc.* 2005; 127:6271. [PubMed: 15853333]
22. Kakwere H, Perrier S. *J Am Chem Soc.* 2009; 131:1889. [PubMed: 19154112]
23. O'Reilly RK, Joralemon MJ, Wooley KL, Hawker CJ. *Chem Mater.* 2005; 17:5976.
24. Hawker CJ, Wooley KL. *Science.* 2005; 309:1200. [PubMed: 16109874]
25. Wang H, Xu J, Wang JH, Chen T, Wang Y, Tan YW, Su HB, Chan KL, Chen HY. *Angew Chem Int Edit.* 2010; 49:8426.
26. Pochan DJ, Chen ZY, Cui HG, Hales K, Qi K, Wooley KL. *Science.* 2004; 306:94. [PubMed: 15459386]

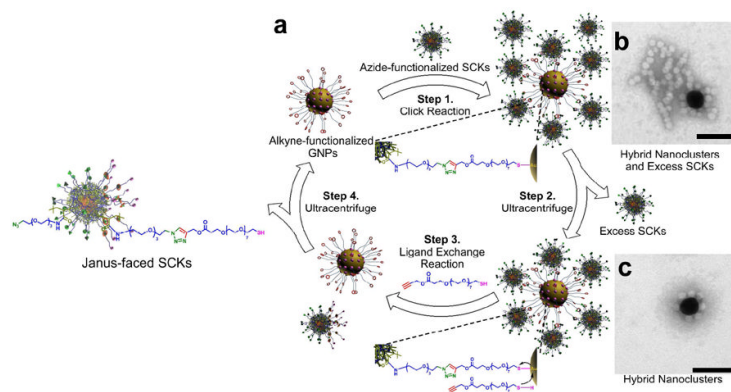


Fig. 1.
a, Schematic representation of the overall strategy. b, TEM image of hybrid nanoclusters, consisting of one GNP surrounded by several SCKs, and an excess of SCKs, after the first step click reaction. c, TEM image of isolated hybrid nanoclusters after removal of unbound SCKs by ultracentrifugation. Scale bars: 100 nm.

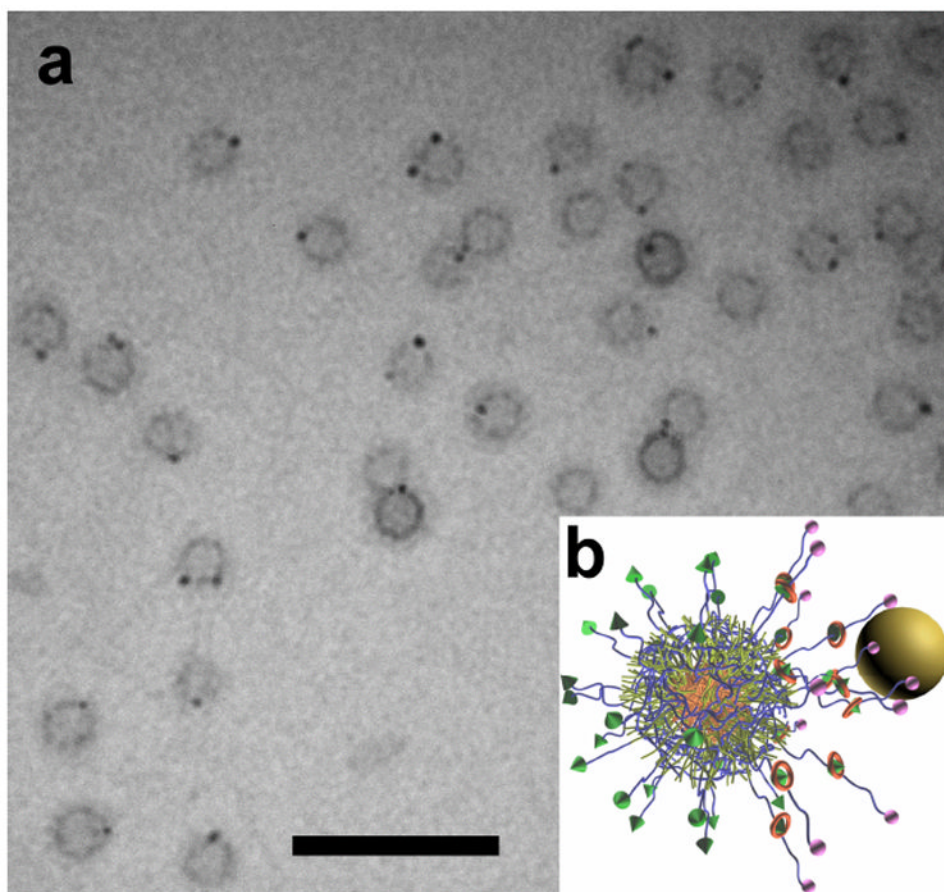


Fig. 2.
a, TEM image of JSCKs labeled with 2 nm GNPs. b, Schematic representation of JSCKs labeled with GNPs. Scale bar: 100 nm.

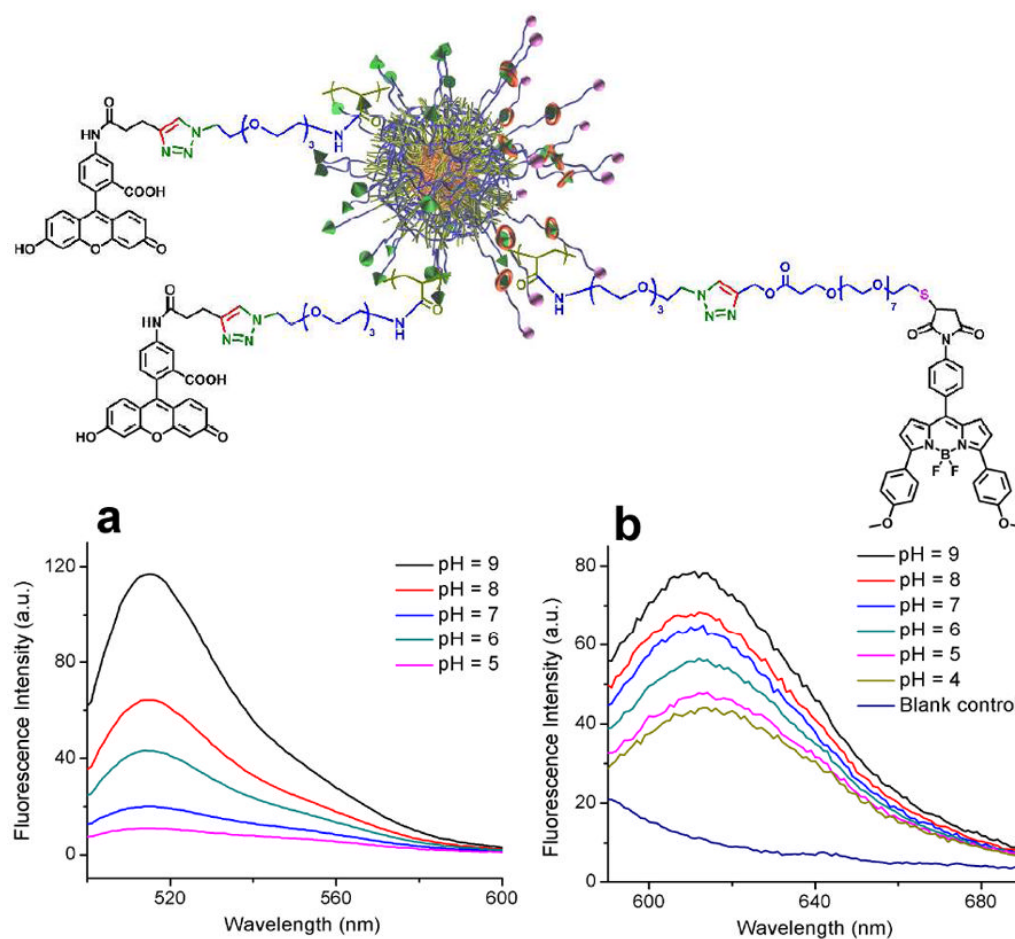
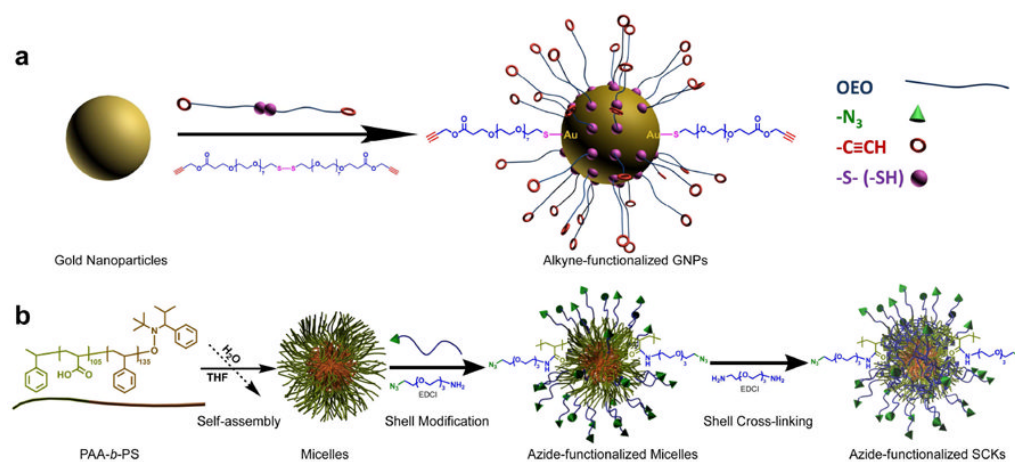


Fig. 3.
 a, pH-dependent fluorescence spectrum ($\lambda_{\text{ex}} = 488$ nm) of JSCKs labeled with alkyne-functionalized fluorescein and thiol-reactive BODIPY 577/618 maleimide, showing the presence of fluorescein. b, pH-dependent fluorescence spectrum ($\lambda_{\text{ex}} = 577$ nm), showing the presence of BODIPY 577/618 maleimide. The chemical structures of each of the conjugated dyes are shown above the corresponding spectra.

**Scheme 1.**

a, Preparation of alkyne-functionalized gold nanoparticle templates. b, Preparation of azide-functionalized SCKs.